Air Quality, Atmosphere & Health (2022) 15:1729–1744
https://doi.org/10.1007/s11869-022-01213-z

Source apportionment of ambient concentration and population exposure to elemental carbon in South Korea using a three-dimensional air quality model

Kyuwon Son[1] · Byeong-Uk Kim[2] · Hyun Cheol Kim[3,4] · Soontae Kim[5]

Received: 13 January 2022 / Accepted: 26 May 2022 / Published online: 29 June 2022

Abstract

We quantified the foreign and domestic contributions to annual mean elemental carbon (EC) concentration over South Korea in 2016 using the Primary Carbon Appointment tool in the community multiscale air quality model. The individual domestic contributions were further examined by emission source category (area, mobile, and point) in each sub-region (i.e., Seoul Metropolitan Area (SMA), Gangwon, Chungcheong, Youngnam, and Honam). EC contribution and population-weighted exposure contribution (PWEC) for each emission source were calculated. Two indicators were compared and adjusted considering uncertainties of emissions from sub-regions. Based on the results of this analysis, the primary EC emission sources that need to be managed to alleviate the concentrations and PWECs were classified, and the cost-effectiveness was compared with contribution rates for EC and PWEC. The modeled annual mean EC concentration in South Korea was 0.6 μg/m^3, of which 54% was contributed by foreign sources (0.3 μg/m^3). However, the quarterly foreign contribution differed by up to five times depending on the monsoon, while the domestic contribution did not. Simultaneously, spatial variations of the annual mean EC contributions are smaller than those of the foreign contributions. Regardless of the uncertainty of emissions, domestic PWEC was 20% higher than the domestic concentration as domestic EC emissions were concentrated in densely populated areas. It implies that EC emission control has more significant meaning not only to improve concentration but also to improve population exposure. In addition, the contribution rate showed greater variation between sub-regions than the EC emission source categories within a region. Considering this, if the cost used to reduce a unit EC emission is the same, the cost effect can be expected when EC emissions are reduced in the sub-regions with a large contribution rate regardless of EC emission source category.

Keywords EC · Source–receptor · Transport · Contribution · Population exposure

Introduction

Elemental carbon (EC)—often interchangeable with black carbon (BC)—is a major component of particulate matter with a diameter equal to or less than 2.5 μm ($PM_{2.5}$) (Poschl 2005; Andreae and Gelencser 2006; Janessen et al. 2011; Petzold et al. 2013). As $PM_{2.5}$ is harmful to human health (Hong and Jo 2003; Lim et al. 2012; Apte et al. 2015; Han et al. 2018), EC can cause adverse health effects, such as lung cancer and respiratory diseases (Morawska et al. 2005; Hart et al. 2009; Rissler et al. 2012, WHO 2012; Lee et al. 2017). Chemically, EC is considered a non-reactive pollutant that can be transported several thousands of kilometers due to its long residence time in the atmosphere (Wolff 1981; Yu et al. 2004; Khan et al. 2006; Shu et al. 2017). Consequently, EC can be used to trace the impact of primary emission sources (Ogren and

✉ Soontae Kim
soontaekim@ajou.ac.kr

1 Department of Environmental Engineering, Ajou University, Suwon 16499, Republic of Korea

2 Georgia Environmental Protection Division, Atlanta, GA 30354, USA

3 Air Resources Laboratory, National Oceanic and Atmospheric Administration, College Park, MD 20740, USA

4 Cooperative Institute for Satellite Earth System Studies, University of Maryland, College Park, USA

5 Department of Environmental and Safety Engineering, Ajou University, Suwon 16499, Republic of Korea

Charlson 1984; Heintzenberg and Winkler 1991). For example, Chen et al. (2013) employed radioactive isotopes to show that approximately 40% of the EC emitted in Beijing and Shanghai in China were transported to South Korea. Similarly, regional contributions of EC emissions in Northeast Asia have previously been estimated using simulation results using three-dimensional photochemical models (Wang et al. 2014; Kim et al. 2017; Liu et al. 2020).

In South Korea, EC accounts for approximately 5–10% of the annual mean $PM_{2.5}$ mass concentrations (Lee and Kang 2001; Kim et al. 2017). While Chinese BC emissions in the 1980s were 8 million tons/year (Qin and Xie 2012; Wang et al. 2016), the amount of BC emissions increased two times in 2009 due to increased BC emissions from industrial and transportation sources (Lu et al. 2019, 2020; Li et al. 2016). In the Clean Air Policy Support System (CAPSS)—the national emissions inventory of South Korea—the amount of annual BC emissions in 2016 was approximately 16,000 tons. Among all emission source categories (defined as area, mobile, and point sources) in CAPSS 2016, the area source was the largest emission source category that accounted for approximately 59% of the total BC emissions in South Korea (Choi et al. 2020; NAIR 2020).

In general, it is crucial to understand major regional and categorical contributors of EC in an area to design effective control strategies to alleviate EC concentrations and population exposure. Studies in northeast Asia have evaluated the health effects of EC only regarding regional or categorical contributors, and not both (Janssen et al. 2011; Peng et al. 2009; Rappazzo et al. 2015; Keuken et al. 2016; Bae et al. 2019; Jia et al. 2020). Moreover, few studies have investigated the effects of long-range transport of EC emissions in northeast Asia as well as domestic contributions in detail by region by emission source category.

Therefore, with air quality simulations, we quantified annual and quarterly contributions of the emission source categories by sub-region to EC concentrations in South Korea as well as foreign sources. As part of the quantitative analysis, we examined population-weighted exposure contribution (PWEC) to identify priority source regions and emission source categories. Lastly, we adjusted PWEC with observed EC concentrations to estimate the extent of EC exposure more accurately. In addition, we distinguished a cost-effective EC emission source for reducing EC concentrations and population exposure using contribution rate. We believe the overall analysis approach taken in this study can be applied to any region that requires efficient EC management strategies.

Materials and methods

Air quality simulation

For the air quality simulations, hourly gridded concentrations for the study period were produced using the Community Multiscale Air Quality (CMAQ) version 4.7.1 (Byun and Schere 2006). Modeling was conducted in 2016 with a 16-day spin-up period from December 16, 2015, to minimize the influence of the initial condition. The simulation domain consisted of 9-km horizontal resolution grids (Fig. 1). A mother modeling domain at a 27-km horizontal grid resolution that covered Northeast Asia, including China, Japan, and South Korea, was used to drive the boundary condition for the 9-km domain (Fig. 1).

SAPRC99 (Carter 1999) and AERO5 (Binkowski and Roselle 2003) were selected as the gas-phase chemical mechanism and the aerosol module, respectively. For meteorological inputs to CMAQ, we used the Meteorology-Chemistry Interface Processor version 3.6 to process simulation results of the Weather Research and Forecasting (WRF) model version 3.4.1. WRF was simulated by dividing each month into two blocks (one block from the 1^{st} to 15^{th} day of each month and the other from the 16^{th} to the last day of each month) for the entire simulation period. All blocks include a 1-day pre-run. Re-analysis data, National Centers for Environmental Prediction-Final (FNL) provided by the National Oceanic and Atomic Administration, were used as initial conditions. Furthermore, to reduce error accumulation during the WRF simulation period, an analysis nudging technique was used for meteorological variables such as winds. This approach was also used in Bae et al. (2022). Model configurations for WRF and CMAQ have been comprehensively summarized in Table 1.

CAPSS 2016 (Choi et al. 2020) and the Comprehensive Regional Emissions Inventory for Atmospheric Transport Experiment 2015 (CREATE 2015) (Jang et al. 2019) were used as the emissions inventories, including EC for South Korea and Northeast countries. The spatial distribution of EC emissions used in this study is shown in Fig. 2. EC emission densities were high over Beijing-Tianjin-Hebei (BTH), Near Beijing (NRB), and Yangtze Reiver Delta (YRD) in China as well as over Seoul Metropolitan Area (SMA), Chungcheong, and Youngnam in South Korea where the population was dense and industries were well developed. The Chinese EC emission of CREATE 2015 used in this study is 1.0×10^6 tons/year; however, in REASv2, 1.1×10^6 tons/year is presented (Kurokawa et al. 2013; Streets et al. 2003). In addition, EC emissions in South Korea were approximately 16,000 tons/year in CAPSS 2016. CAPSS 2017, an updated national emission inventory of South Korea, estimated that EC emissions in South Korea is 15,600 tons, i.e., 5% smaller than that in CAPSS 2016 (NAIR, 2022). The emission inventory was further processed through spatiotemporal allocation and chemical speciation processes with the Sparse Matrix Operator Kernel Emissions (SMOKE) model to prepare hourly gridded inputs for the air quality simulation (Kim

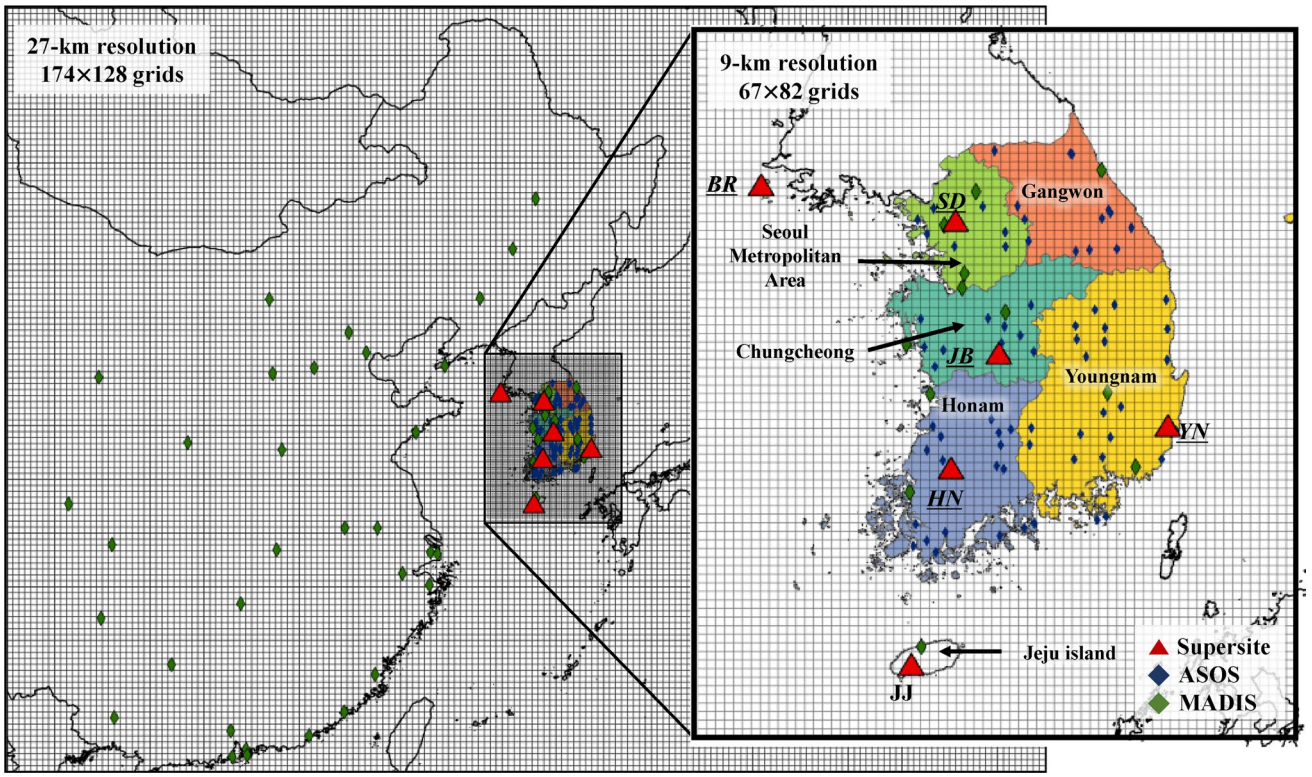

Fig. 1 Coarse (27 km) and fine (9 km) modeling grid domains used in this study and the five tagged sub-regions (Seoul Metropolitan Area, Gangwon, Chungcheong, Youngnam, and Honam). Red triangles represent the locations of supersites: Baengnyeong (BR), "Sudo" for Seoul Metropolitan Area (SD), Jungbu (JB), Honam (HN), Youngnam (YN), and Jeju (JJ). Navy and green diamonds represent the locations of 72 ASOS and 59 MADIS sites, respectively

Table 1 Configurations for WRF and CMAQ models used in this study

WRF	Option	CMAQ	Option
Version	3.4.1	Version	4.7.1
Source of initial and boundary conditions	FNL	Chemical mechanism	SAPRC99
PBL scheme	YSU	Aerosol module	AERO5
LSM scheme	NOAH Land	Advection scheme	YAMO
Microphysics	WSM6	Initial and Boundary conditions	Profile ICON BCON extracted from 27-km domain runs by Kim et al. (2020)

et al. 2008). The top three emission types in SMOKE processed EC emissions by source category are represented in Table S1.

Model performance evaluation

Meteorological model performance

For meteorological model performance evaluation, we used observational data from 72 automated surface observing systems (ASOS) sites available in South Korea. In addition, meteorological data at meteorological assimilation data ingest system (MADIS) sites in China and South Korea based on a 27-km resolution simulation was used to interpret quarterly domestic and foreign EC contributions considering the regional-scale meteorology. We also evaluated the performance of the meteorological model at 26 and 33 MADIS sites in South Korea and China, respectively. The locations of 72 ASOS sites and 59 MADIS sites are provided in Fig. 1. The modeling

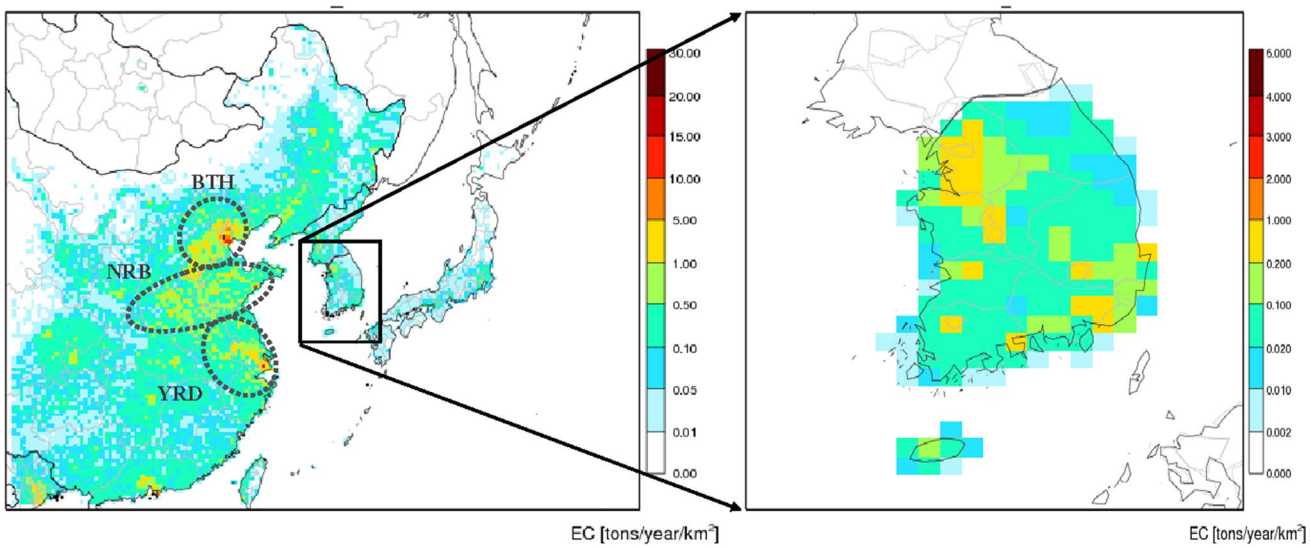

Fig. 2 Annual elemental carbon (EC) emission densities (tons/km^2) over Northern Asia (left) and South Korea (right) as reported in CREATE 2015 and CAPSS 2016 that are used in this study

error and consistency between the observed and simulated results were estimated using the root mean square error (RMSE) and index of agreement (IOA) values, respectively, at the observation sites. The RMSE was calculated as a difference between the average of simulated (M_i) and observed (O_i) daily mean value and the number of days in target period (n) (Eq. 1). The IOA was computed with the components used to calculate RMSE and the average of the observed daily mean value (O) (Eq. 2).

$$\text{Root mean square error} = \sqrt{\frac{\sum_{i=1}^{n}(M_i - O_i)^2}{n}} \tag{1}$$

where,

n : Number of days in the target period.

M_i : Simulated daily mean value in the i^{th} day.

O_i : Observed daily mean value in the i^{th} day.

$$\text{Index of Agreement} = 1 - \left[\frac{\sum_{i=1}^{n}(O_i - M_i)^2}{\sum_{i=1}^{n}(|M_i - \text{O}| + |O_i - \text{O}|)^2}\right] \tag{2}$$

where,

M_i : Simulated daily mean value in the i^{th} day.

O_i : Observed daily mean value in the i^{th} day.

O : Average of the observed daily mean value.

Air quality model performance

The simulated EC concentrations were evaluated at six supersites in South Korea for the air quality model performance with normalized mean bias (NMB) and normalized mean error (NME). NMB and NME are indicators of over-/underestimation and uncertainty in simulation results, respectively. These two performance statistics are recommended as benchmark indices for evaluating EC simulations (Emery et al. 2017). In this study, the definitions of NMB and NME follow the definitions used by Emery et al. (2017). NMB and NME are performance indicators usually used in air quality model evaluations and were recommended as one of the six evaluation factors for air quality model evaluation in Huang et al. (2021). In this study, the NMB and NME were determined using the simulated daily mean EC concentration and the observed daily mean EC concentration for each supersite (Eq. 3 and Eq. 4). Consequently, 366 concentration data (n) were used to calculate the NMB and NME for the study period. Results of the air quality model performance evaluation are presented in the "Air quality model performance evaluation" section.

$$\text{Normalized mean bias (\%)} = \sum_{i=1}^{n}\frac{(M_i - O_i)}{O_i} \times 100(\%) \tag{3}$$

$$\text{Normalized mean error (\%)} = \sum_{i=1}^{n}\frac{|M_i - O_i|}{O_i} \times 100(\%) \tag{4}$$

where,

n : Number of days in the target period.

M_i : Simulated daily mean EC concentration in the i^{th} day (μg/m^3).

O_i : Observed daily mean EC concentration in the i^{th} day (μg/m^3).

Contribution analysis

The Primary Carbon Apportionment (PCA) of the CMAQ was used to analyze the source–receptor relationship for EC in this study (Emery et al. 2017). We used the source allocation approach (Thunis et al. 2018) to identify the major EC emission sources at a sub-category level as follows. First, we quantified the EC contribution by source category using the CMAQ-PCA simulation. Later, sub-categorical EC contributions were estimated comprehensively by multiplying the categorical EC contribution with the emission ratio of a targeted sub-categorical source.

The total number of tagged emission sources was 15: three emission source categories (area, mobile, and point emission sources) for each of 5 sub-regions of South Korea—SMA, Gangwon, Chungcheong, Youngnam, and Honam. We did not include some islands, such as Jeju, as part of "South Korea" or "domestic" areas in this study for the purpose of simplicity because the amount of annual BC emissions from Jeju Island accounted for only 2% of the total BC emissions from South Korea in CAPSS 2016; moreover, Jeju is geographically far from the mainland. The tagged five sub-regions are shown in Fig. 1.

For the contribution analyses, the domestic contribution was further classified into two groups: (1) "self" contribution by emissions within a sub-region and (2) contribution by emissions in "the other sub-regions," i.e., the domestic contribution excluding self-contribution. In turn, the total EC concentrations in a sub-region, excluding the domestic contribution, were treated as "foreign contribution" (Fig. 3). Therefore, the foreign contribution in this study includes the contributions by boundary conditions and the Jeju Island.

Evaluation of source-specific population exposure

Although EC has a lower concentration than inorganic $PM_{2.5}$ components (sulfate, nitrate, ammonium), it has 2 to 10 times the mortality of $PM_{2.5}$ (Krall et al. 2013). In addition, EC concentration is known to be proportional to $PM_{2.5}$ concentration (Dao 2022; Feng et al., 2009; Zhang et al. 2012). Furthermore, as the health effects of $PM_{2.5}$ vary depending on their composition (Cao et al. 2012; Li et al. 2019; Qiao et al. 2014), it is necessary to prioritize the evaluation of health effects for $PM_{2.5}$ components (McMurry et al. 2004). Thus, in this study, the population exposure to EC was calculated in consideration of the health risk of EC.

To examine the exposures level of EC contributions in South Korea by source category considering population of each sub-region, we used the PWEC. The advantages of PWEC in highlighting the significance of specific emission sources in actual population exposure over an area have been demonstrated in previous studies (Aunan et al. 2018; Son et al. 2020; Bae et al. 2021). As defined in Eq. (6), PWEC (expressed in μg/m^3) of an emission source category k located in a sub-region j, $PWEC^{j,k}$, is a value resulting from dividing a sum of the products of $C_i^{j,k}$ and the population of a sub-region i, P_i, by the sum of P_i. A higher PWEC indicates that a source likely contributes to higher population exposure to the airborne EC.

$$PWEC^{j,k}(\mu g/m^3) = \frac{\sum_{i=1}^{n}(C_i^{j,k} \times P_i)}{\sum_{i=1}^{n} P_i} \quad (5)$$

where,

$PWEC^{j,k}$: Population-weighted exposure contribution by the emission source category k within the source sub-region j (μg/m^3).

$C_i^{j,k}$: Modeled EC contribution by the emission source category k within the sub-region j to a receptor sub-region i (μg/m^3).

P_i : Population of a receptor sub-region i (persons).

Results and discussion

Model performance evaluation

Meteorological model performance evaluation

During 2016, the simulated annual mean 10-m wind speeds at the 72 ASOS sites in South Korea was 3.1 m/s and the RMSE and IOA were 1.2 m/s and 0.8, respectively.

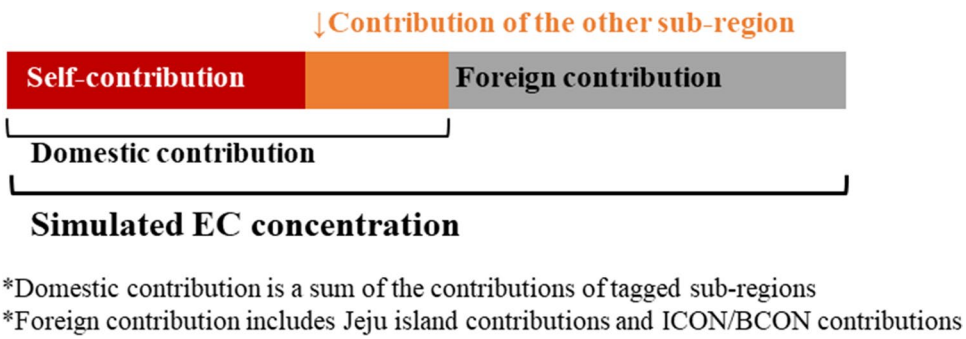

Fig. 3 Illustrative relationship between a simulated EC concentration in a sub-region and the contributions analyzed in this study

Compared to the recommended benchmarking value for biases proposed by Emery et al. (2001), the values of RMSE and IOA for 10-m wind speeds were within the recommended value range at the ASOS sites. For 2-m temperatures, the simulated annual mean value at the ASOS sites in South Korea was 13.0 ℃. Moreover, the IOA (1.0) was satisfactory regarding the benchmarking values recommended by Emery et al. (2001) (Table 2). Evaluation of the meteorological model performance using MADIS data showed that the 10-m wind speed in South Korea had an RMSE of 0.56 m/s and IOA of 0.93. The meteorological model performance evaluation result of 2-m temperature at the MADIS sites in South Korea showed that RMSE and IOA were 1.16 ℃ and 1.0, respectively. Furthermore, RMSEs of 10-m wind speed and 2-m temperature at Chinese MADIS sites were 0.37 m/s and 0.6 m/s, respectively, and the IOA was 0.91 and 1.00, respectively. Therefore, the result of the meteorological model performance evaluations at the MADIS sites over South Korea and China met the benchmarking goal of Emery et al. (2001). In addition, the results of daily model performance evaluation and quarterly spatial model performance evaluation of 10-m wind speed, 2-m temperature, and surface pressure at MADIS sites in South Korea and China are presented in Figure S2.

Air quality model performance evaluation

The highest annual mean EC concentration was observed at the JB (1.3 μg/m^3) supersite, followed by the SD (1.2 μg/m^3), HN (1.2 μg/m^3), JJ (0.9 μg/m^3), BR (0.9 μg/m^3), and YN (0.6 μg/m^3) supersites during 2016. For the same period, the simulated annual mean EC concentrations were 0.2 μg/m^3 higher than the observed concentrations at the SD and YN supersites while 0.3, 0.5, 0.2, and 0.6 μg/m^3 lower at the BR, JB, HN, and JJ supersites, respectively (Fig. 4). The NMB and NME for daily mean EC concentrations at the six supersites during the study period ranged from − 58% (JJ) to 28% (YN) and from 34% (SD) to 59% (JJ), respectively. The correlation coefficient (r) between the modeled and observed daily mean EC concentrations ranged from 0.58 (JJ) to 0.72 (BR). Table 3 shows the comprehensive results of the performance statistics.

Table 2 Model performance statistics for 10-m wind speeds and 2-m temperatures at 72 ASOS sites in South Korea, 26, 33 MADIS sites in South Korea and China, respectively

South Korea @ ASOS	Observation	Simulation	RMSE	IOA
10-m wind speeds	2.02 m/s	3.06 m/s	1.21 m/s	0.77
2-m temperature	13.52 ℃	12.99 ℃	1.26 ℃	1.00
South Korea @ MADIS	Observation	Simulation	RMSE	IOA
10-m wind speeds	2.62 m/s	2.94 m/s	0.56 m/s	0.93
2-m temperature	13.20 ℃	12.63 ℃	1.16 ℃	1.00
China @ MADIS	Observation	Simulation	RMSE	IOA
10-m wind speeds	3.00 m/s	3.11 m/s	0.37 m/s	0.91
2-m temperature	15.95 ℃	15.77 ℃	0.60 ℃	1.00

Performance goals for 10-m wind speeds by Emery et al. (2001): RMSE ≤ 2 m/s and IOA ≥ 0.6

Performance goals for 2-m temperatures by Emery et al. (2001): IOA ≥ 0.7

Uncertainties in emissions inventory

Simulation uncertainty results from the uncertainties in emission and meteorological data as well as other input data for the simulation (Jo et al. 2017; Kim et al. 2017; Mun et al. 2017). For this study, as the model performance evaluation for meteorological simulation met the benchmarking goals suggested by Emery et al. (2001), as described in the "Meteorological model performance evaluation" section, we assumed that the uncertainty of the simulated EC concentrations mainly originated from the uncertainty of EC emission inventory. The uncertainty of emission inventory includes uncertainties of foreign and domestic emissions. Therefore, we adopted a two-step approach to adjust the foreign and domestic EC contributions. In the first step, as the BR supersite is known to represent the effect of foreign emissions according to previous studies (Sung et al. 2017; Kim et al. 2021), the foreign contribution at each supersite was adjusted by dividing the ratio, 0.64, of simulated and observed EC concentration at the BR supersite (Table 3). The performance of simulated EC concentrations at the BR supersite met the performance goal proposed by Emery et al. (2017). In the second step, we treated the adjusted domestic EC contribution as the gap between the observed EC concentration and the adjusted EC foreign contribution. In addition, we assumed that the ratio of domestic contributions before and after adjustment at each supersite is equal to EC emission uncertainty in the sub-region where the supersite belongs. As a result of the adjustment, EC emissions in SMA and Youngnam were overestimated at 49% and 59%, respectively, whereas those in Chungcheong and Honam were underestimated at 55% and 13%, respectively. In the subsequent sections, we analyzed EC exposure contributions not only by weighing the population of sub-regions but also by adjusting modeling uncertainties.

EC contributions by foreign and domestic sources

The average annual EC concentration for each sub-region was in the range of 0.2 μg/m^3 (Gangwon) to 0.6 μg/m^3 (SMA), and the fraction of EC in $PM_{2.5}$ was in the range

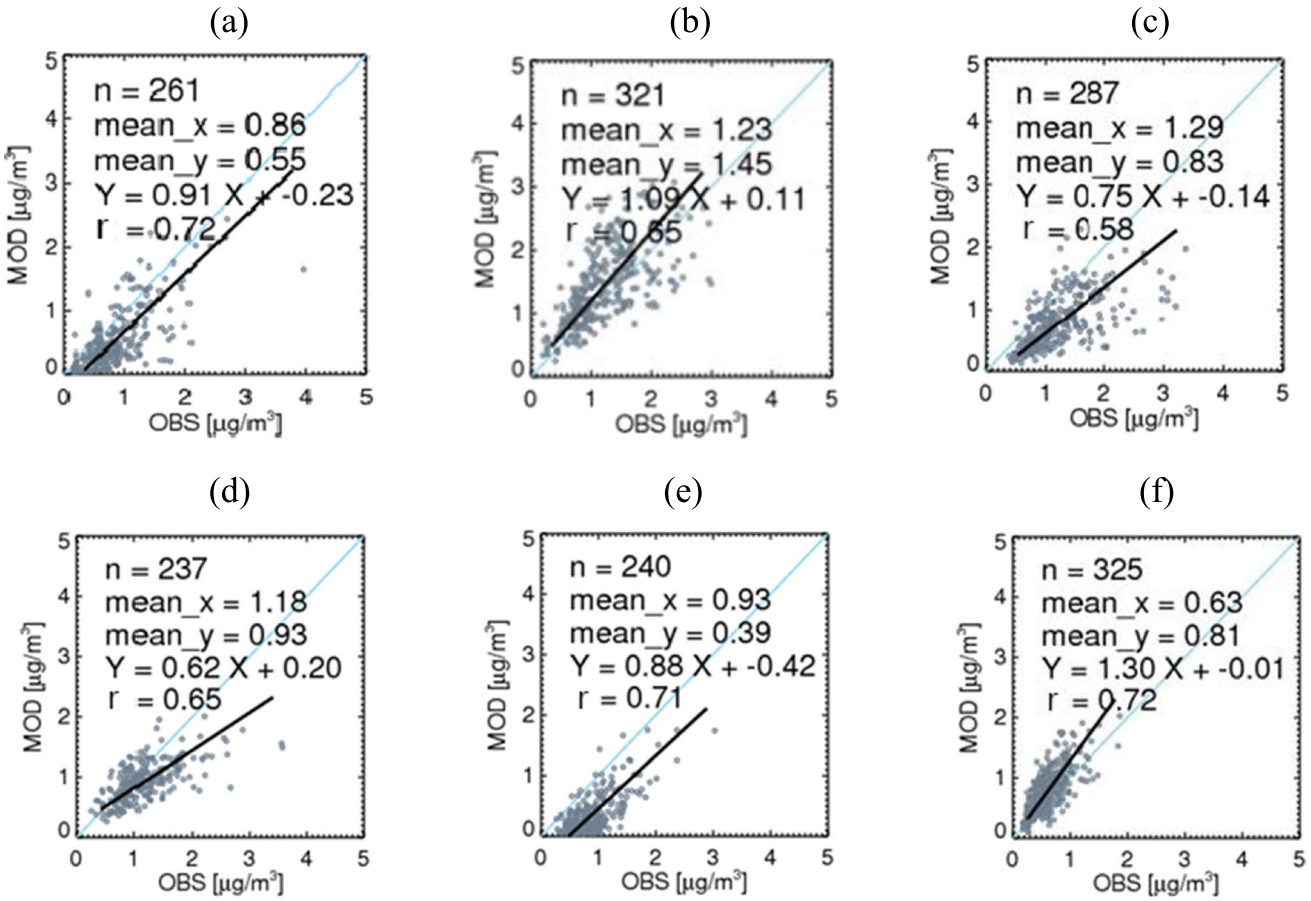

Fig. 4 Scatter plots of daily mean observed and simulated EC concentrations at the **a** BR, **b** SD, **c** JB, **d** HN, **e** JJ, and **f** YN supersites

of 5% (Honam) to 8% (SMA) (Fig. 5a). Also, the $PM_{2.5}$ concentration in the sub-region with the high fraction of EC was also high. This suggests that the importance of EC increases with the increasing $PM_{2.5}$ concentration in South Korea. The domestic contributions to spatially averaged annual mean EC concentrations in individual sub-regions varied among sub-regions, ranging from 0.2 μg/m^3 (Gangwon) to 0.6 μg/m^3 (SMA) while the annual mean foreign EC contribution showed marginal variations, ranging from approximately 0.3 μg/m^3 (Youngnam) to 0.4 μg/m^3 (SMA), as shown in Fig. 5b and c. Overall, the foreign contribution to the annual mean EC concentration over all sub-regions in South Korea was slightly higher than the domestic contribution except some places where the EC emission densities were high (e.g., the southern of SMA, the northeastern of Chungcheong, and the southeastern of Youngnam) as shown in Fig. 5b and c. These high EC emission density areas, where the domestic contribution was higher than the foreign contribution to the EC concentration in South Korea, accounted for large portions of EC emissions in the corresponding sub-regions: 53% of SMA, 42% of Chungcheong, and 43% of Youngnam.

Table 3 Performance statistics for modeled EC concentrations at the six supersites in South Korea. Values in the bold font indicate model performance at specific supersites met the performance goals for 24-h EC proposed by Emery et al. (2017)

	Observation (μg/m^3)	Simulation (μg/m^3)	NMB (%)	NME (%)	*r*
BR	0.86	0.55	−35.90	43.10	0.72
SD	1.23	1.45	17.96	34.21	0.65
JB	1.29	0.83	−35.90	39.83	0.58
HN	1.18	0.93	−20.78	28.21	0.65
JJ	0.93	0.39	−57.80	58.65	0.71
YN	0.63	0.81	27.81	38.20	0.72

Performance goals for 24-h EC by Emery et al. (2017): −20% ≤ NMB ≤ 20%, NME ≤ 50%

However, the domestic and foreign EC contributions presented in this study were based on the emissions inventory and were subject to uncertainties described in the "Uncertainties in emissions inventory" section. In addition, the domestic and foreign EC contributions would be different from the results of this study if a different or improved

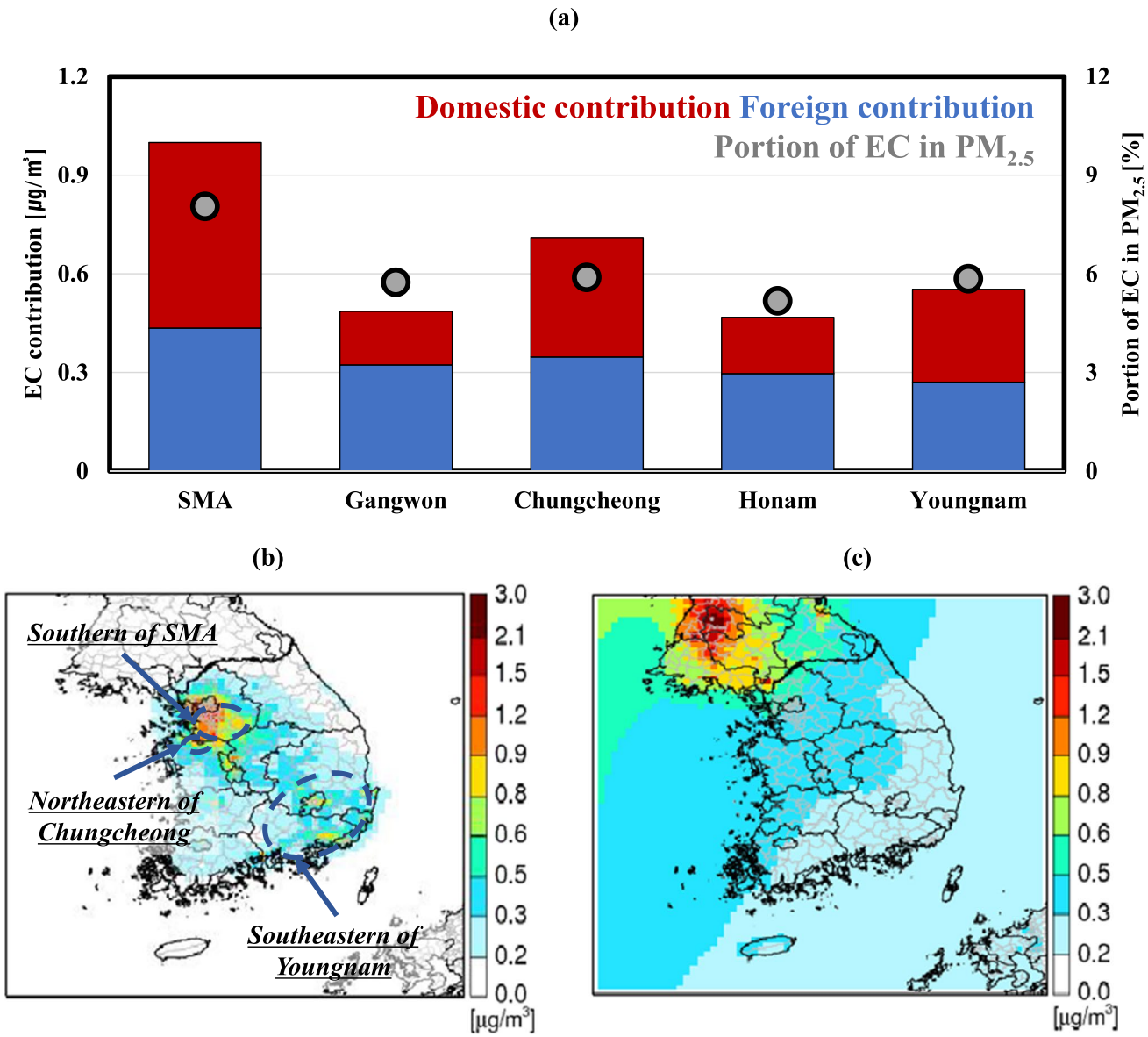

Fig. 5 **a** Annual mean EC contributions from foreign and domestic emissions and the fraction of EC in $PM_{2.5}$ over five sub-regions in South Korea; and spatial distributions of **b** domestic and **c** foreign EC contributions

emissions inventory were used. Therefore, in this study, we selected a simple adjustment approach to reflect model uncertainties based on observation data (see the "EC population exposure" section for details). However, a more robust method to correct domestic and foreign regional EC emissions inventories and to reflect corresponding changes in EC contributions will be needed in the future.

The EC concentrations and the EC emission densities across sub-regions show a linear trend with a high correlation coefficient (0.94) as shown in Fig. 6. A statistical significance test was performed to prove that the linear relationship between sub-regional EC concentrations and the EC emission densities are not by chance. The *t*-test result showed that the *p*-value was approximately 0.05 by sub-region and less than 0.05 by provincial authority (significance level: $p < 0.05$) (Table S2). The fact that the *p*-value is less than 0.05 proved that the EC emission density and EC concentration by region had a linear relationship by rejecting the null hypothesis; i.e., the slope of the trend line is 0, with the *t*-test. The 95% confidence intervals for the slope and *y*-axis intercept value of the trend line by sub-region were [0.91, 2.14] and [0.37, 0.39], respectively. Moreover, the EC concentration and emission density of 17 provincial authorities that is one jurisdictional level lower than sub-regions also showed a high correlation coefficient (0.82). Thus, the high correlation between primary air pollutant

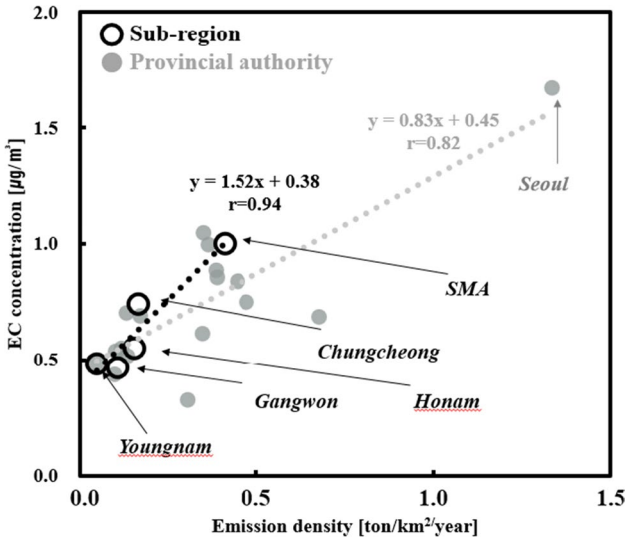

Fig. 6 Correlations between simulated annual mean EC concentrations and EC emission densities of sub-regions (black) and provincial authorities (gray) over South Korea during the simulation period

concentration and its emission density was reported by previous studies (Fisher and Sokhi 2000; Kiesewetter et al. 2013; Kim et al. 2020).

It was also reported that the deviation of the sub-regional EC contributions from foreign emissions was smaller than that from local EC emissions in previous studies (i.e., Jeong et al. 2011, 2011; Xing et al. 2020) and is shown here. This means that sub-regional EC concentrations are more sensitive to the impact of their own EC emissions as compared to long-range transported EC concentrations. Meanwhile, as reported in previous studies (i.e., Feng et al. 2014; Gu et al. 2010; Sahu et al. 2011; Wang et al., 2018), the diurnal concentration variation of air pollutants represents the effect of local emissions. The diurnal EC concentrations observed at the SD, JB, HN, and YN supersites belonging to the five sub-regions were remarkable, especially the foreign contributions were uniform during the whole day, but the domestic contributions increased during rush hour (Figure S3). It means that difference between local EC emissions can cause difference between sub-regional EC concentrations.

Simultaneously, the EC contributions from EC emission densities by each sub-region or each provincial authority could be estimated by multiplying the slope of trend line and emission densities. The estimated EC contributions from EC emissions by each sub-region or by each provincial authority ranged from 0.1 μg/m^3 (Gangwon) to 0.6 μg/m^3 (SMA), and from 0.0 μg/m^3 (Jeju) to 0.9 μg/m^3 (Seoul), respectively. Therefore, the trend line for sub-regional EC emission density and EC concentration can be used to roughly estimate the EC contribution from the sub-regional emission. We also noted that the *y*-intercept in Fig. 6 did not reach zero.

As the meteorology and emission changed with time, we examined temporal variations of domestic and foreign EC contributions over five sub-regions. For this analysis, we divided the year into four quarters: January–March as Q1, April–June as Q2, July–September as Q3, and October–December as Q4. The quarterly domestic contributions averaged across five sub-regions ranged from 0.3 μg/m^3 (Q2) to 0.4 μg/m^3 (Q4) while foreign contributions varied from 0.1 μg/m^3 (Q3) to 0.6 μg/m^3 (Q1) (Fig. 7). Differences in minimum and maximum quarterly EC contributions were 0.1 μg/m^3 for domestic sources and 0.5 μg/m^3 for foreign sources. In particular, the foreign EC contributions increased during Q1 and Q4 when temperatures were relatively low (Figure S1). This is because the northwesterly wind prevails in South Korea due to monsoons in Northeast Asia during these quarters (Figure S1 and Figure S4). The foreign EC contributions in SMA and Chungcheong located in the northwest of South Korea during Q1 and Q4 are higher than those in other sub-regions. This analysis result supports a strong relationship between prevailing wind pattern and foreign contribution in certain quarters. In addition, the backward trajectory analysis with Hybrid Single-Particle Lagrangian Integrated Trajectory indicated that air masses reaching South Korea likely originated from Liaoning and BTH in China during Q1 and Q4, while multiple origins (including the Northern Pacific and Japan) of long-range transported air masses were observed during Q2 and Q3 (Figure S5). However, consistent quarterly domestic EC contributions imply that EC emission reduction in South Korea will be effective in alleviating EC concentrations relatively independent of the quarterly variations of meteorology and emissions. It was also noted that spatial variations of domestic EC contributions are relatively larger than those of the foreign contributions, although in seasonal variations the opposite condition holds (Figure S6).

EC contributions by sub-region and source category

The averaged domestic contribution to EC concentration in each sub-region was 0.28 μg/m^3 while the average self-contribution by all sub-regions was 0.20 μg/m^3 (approximately 70% of the domestic contribution). The averaged contribution from the other sub-regions was about a half of self-contribution when averaged over South Korea (Fig. 8a). Self-contributions by each sub-region ranged from 0.06 μg/m^3 (13%, Gangwon) to 0.48 μg/m^3 (48%, SMA) (Fig. 8b–f and Table S3). Thus, we inferred that managing EC emissions from a sub-region by itself is more important than managing those from the other sub-regions to reduce EC concentrations in the sub-region. The

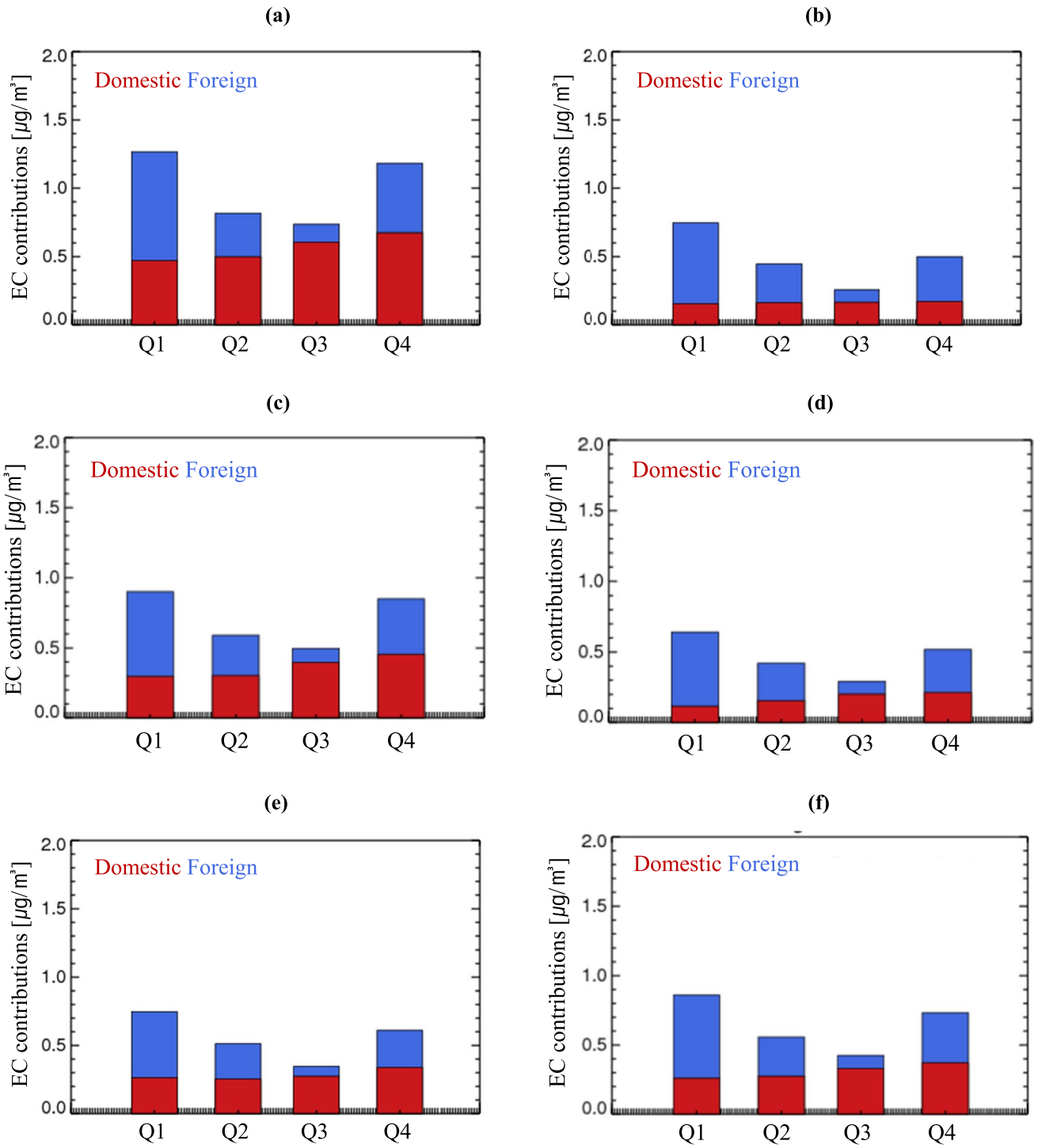

Fig. 7 Quarterly domestic (red) and foreign (blue) EC contributions at **a** Seoul Metropolitan Area (SMA), **b** Gangwon, **c** Chungcheong, **d** Youngnam, **e** Honam, and **f** averaged across five sub-regions

exception is Gangwon: the contribution of the other sub-regions for Gangwon was approximately 1.5 times the self-contribution of Gangwon. Especially, the EC contribution by SMA (where EC emission density was eight times that of Gangwon) to EC concentrations of Gangwon was 1.2 times the self-contribution by Gangwon. The relative contribution ratios of area, mobile, and point emission source categories in South Korea were 20:10:1 (Figure S7) that was similar to their EC emission ratios, which reflects a linear correlation between emissions and the concentrations of primary air

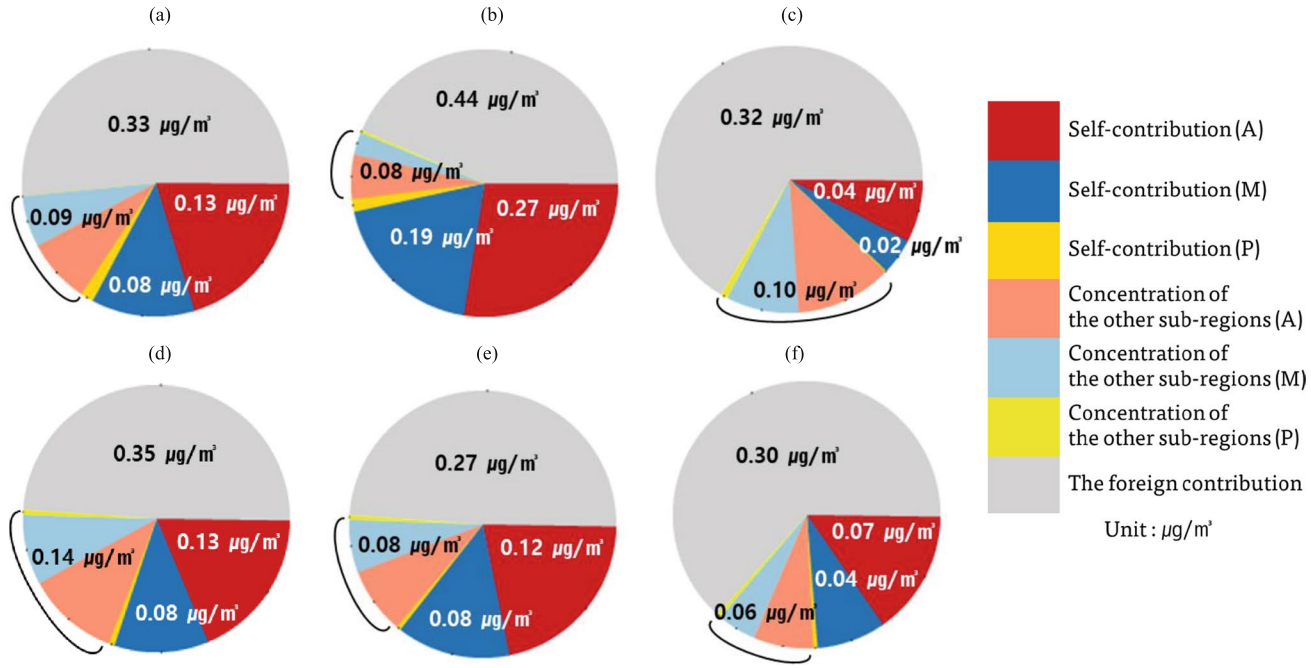

Fig. 8 Pie charts of simulated annual mean EC concentrations by self-contributions, contributions by the other sub-regions, and the foreign contributions over (**a**) the average of five sub-regions, (**b**) SMA, (**c**) Gangwon, (**d**) Chungcheong, (**e**) Honam, and (**f**) Youngnam. The black bracket indicates a sum of contributions by all source categories from the other sub-regions

pollutants. Therefore, we concluded that managing areas and/or mobile sources should be prioritized over managing point sources in South Korea. Among the area and mobile sources, Table S1 shows that off-road mobile sources, on-road mobile sources, and bio-combustions were the most significant sub-categorial sources that further investigations for feasible control measures on these source categories are necessary for South Korea.

EC population exposure

We estimated the population exposure by each emission source category using the EC contributions calculated through the air quality simulation. Here, the EC contribution and population exposure were initially calculated based on emissions inventory and then further adjusted with EC emission uncertainty at each sub-region, as described in the "Uncertainties in emissions inventory" section. That is, adjusting concentrations and PWECs can alleviate over-/underestimates of the EC concentrations in sub-regions caused by emission uncertainties, as explained in the "Uncertainties in emissions inventory" section. Uncertainty in the foreign EC emissions that affect long-range transport was estimated using the ratio of observed and simulated EC concentrations at the BR supersite. In addition, among the five sub regions, Gangwon was excluded from the adjustment to contribution and PWEC as no observed EC concentration data were available.

As shown in Fig. 9, the domestic contribution to the EC concentration averaged over all sub-regions was 0.29 μg/m^3 and 0.23 μg/m^3 before and after adjustment, respectively. Both values were lower than the foreign contribution (0.33 μg/m^3). Before adjustment, the domestic PWEC (0.41 μg/m^3) was higher than the foreign PWEC (0.37 μg/m^3). However, domestic PWEC decreased to 0.28 μg/m^3 after adjustment (Fig. 9b) due to decreasing PWEC in SMA and Youngnam where EC contribution decreased after adjustment. As SMA and Youngnam have relatively large populations among the five sub-regions, the fluctuation of domestic PWEC is heavily influenced by emission uncertainties of these sub-regions. Nevertheless, the risk from domestic and foreign emissions was higher irrespective of emission adjustment when expressed in terms of PWEC rather than contribution. It implies that the EC concentrations are high in densely populated areas. Therefore, alleviating EC concentrations in highly populated areas may need to be high in air quality management priorities.

Furthermore, we calculated a contribution rate for EC and population exposures due to each EC emission source category. In this study, the contribution rate for EC and population exposure by EC emission source category was defined as the adjusted EC contribution and PWEC is described in Fig. 9 per unit EC emissions of each EC emission source category, respectively. The concept of contribution rate is similar to

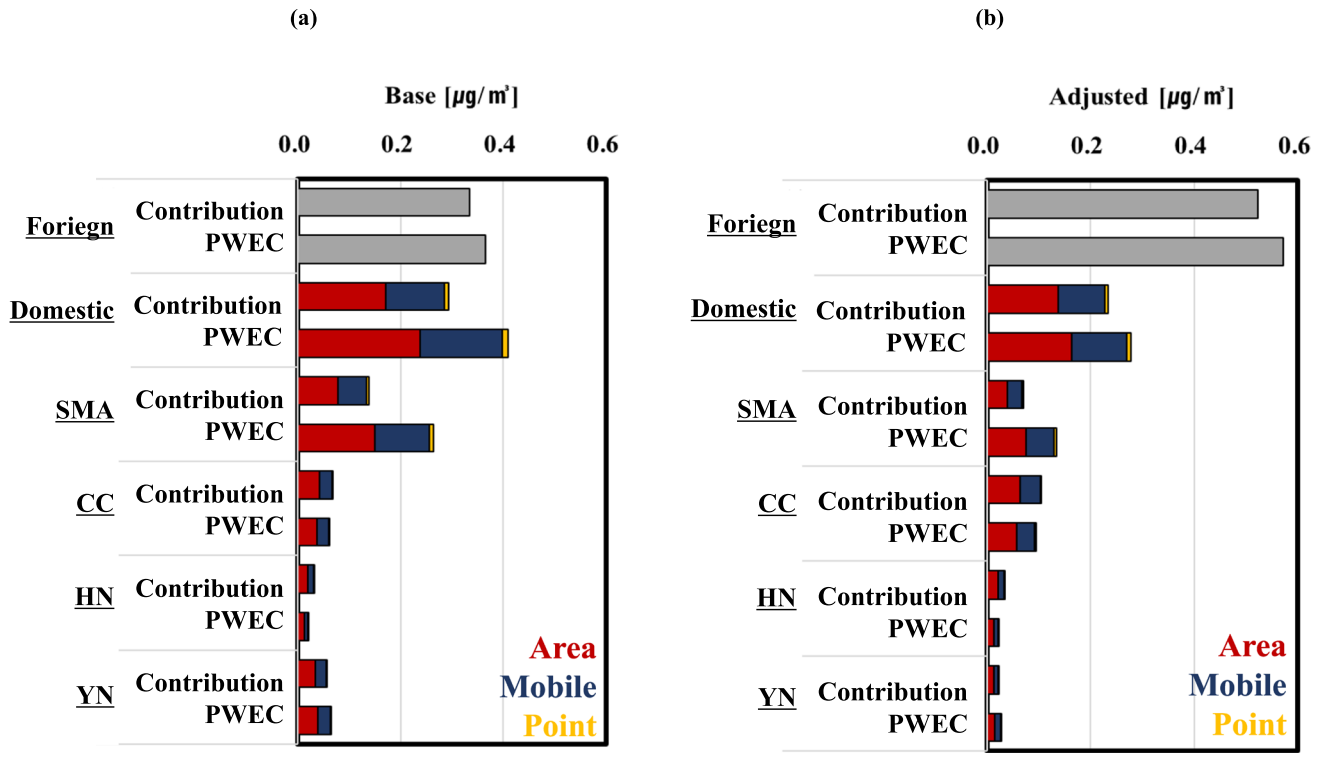

Fig. 9 Comparisons with concentrations and population-weighted exposure contributions (PWECs) for **a** base modeling and **b** modeling with adjusted emissions for foreign areas and four sub-regions (SMA, Chungcheong, Honam, and Youngnam) in South Korea during the simulation period of 2016. "Domestic" indicates the contribution and PWEC of South Korea excluding Gangwon. Red, blue, and yellow bars represent the contributions from area, mobile, and point source categories in South Korea, respectively

that of conversion rate, which is defined as concentration per unit emission. The conversion rate was used in many previous studies (Kim et al. 2017; Pierson et al. 1979; Tang et al. 2020; Viatte et al. 2021). If the cost of unit EC emission reduction is the same, managing EC emissions with a large contribution rate for EC or PWEC will be cost-effective. Thus, contribution rate is a helpful index to distinguish certain EC emission source categories to efficiently reduce EC exposure.

For 12 EC emission source categories, the average contribution rate for PWEC was approximately 5% higher (0.019 μg/m^3/g/year) than that for EC (0.018 μg/m^3/g/year). It implies that EC emission management has significance in reduction for both simple EC concentration and population exposure. When EC emission sources are located in densely populated areas, the high population exposure to EC is expected. In particular, the contribution rate for EC, averaged across all emission source categories in the densely populated SMA, was 0.014 μg/m^3/g/year while the contribution rate for PWEC was 0.026 μg/m^3/g/year (Fig. 10). In contrast, the difference in contribution rates for EC and that for PWEC by emission source categories within a sub-region were minimal, while contribution rates for EC contribution or PWEC can differ up to 10 times by sub-regions. Therefore, to reduce EC concentrations and population exposure to EC, it is necessary to manage EC emission sources in the order of regions rather than emission source category with high conversion rates if the cost of reducing EC emissions by region is the same.

Conclusion

This study analyzed the contribution of foreign EC emissions and the domestic contributions of three EC emission source categories to EC concentrations over South Korea in 2016. The simulated annual mean EC concentration in South Korea was 0.6 μg/m^3, and the foreign contribution (54%) was higher than the domestic contribution (46%). Furthermore, the variation of annual mean domestic EC contributions by sub-region was larger than that of foreign contributions. During Q1 and Q4, the northwesterly wind blew strongly due to the influence of monsoons, increasing the foreign contribution by up to 5 times, while the quarterly difference in domestic contribution was minimal. This suggests that EC concentration in each sub-region has a high correlation with EC emission density in its own sub-region, although the EC concentrations are also determined by various factors such as transport process

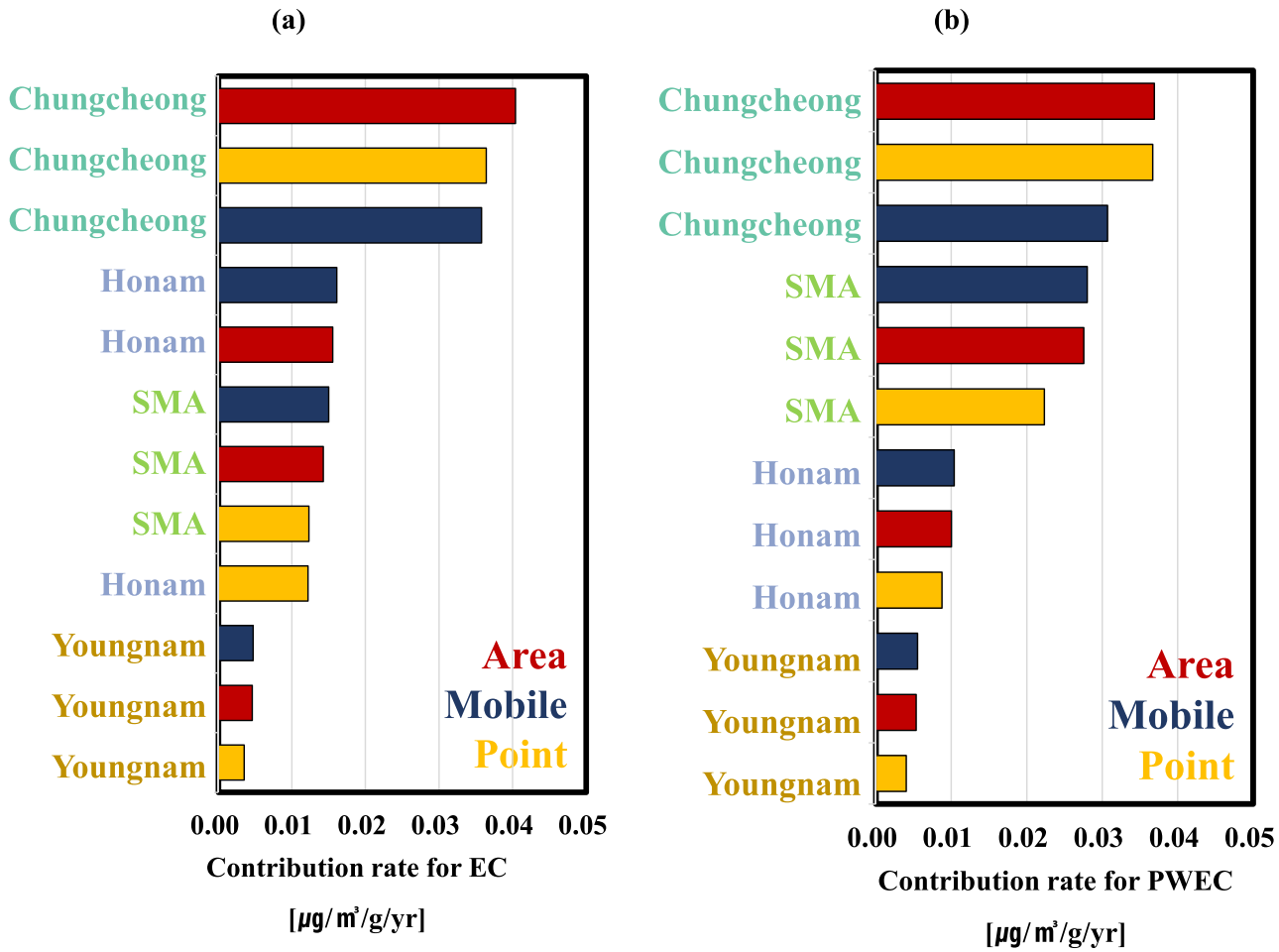

Fig. 10 Sub-region EC emission contribution rates for **a** annual mean EC and **b** PWECs by emission sources. Each sub-regional EC contribution and PWEC used to calculate contribution rate in this figure is the adjusted value represented in Fig. 9

and meteorological characteristics. Among the domestic contributions, the self-contribution in the five sub-regions of South Korea, excluding Gangwon, was twice as high as that of the other sub-regions. Therefore, EC emission management in self region can effectively reduce the EC concentrations in the region.

The present study showed that the adjusted domestic PWEC (0.3 μg/m^3) was approximately 20% higher than adjusted domestic contribution (0.2 μg/m^3). In addition, the domestic contributions were spatially highly variable in all areas, including densely populated areas. This suggested that the management of domestic EC emissions is important to improve not only air quality but also population exposure. In general, combining the contributions of source categories and the emission amounts of the major emission types can shed light on what emission sources should be controlled first to improve EC concentration and exposure over the region of interest. In addition, we suggest that the sub-regions with a large contribution rate for EC or PWEC would be most effective in terms of cost-effectively improving population exposure and air quality in South Korea.

However, we also noted the differences between the EC contribution based on the published emission inventory and the adjusted contributions in each sub-region. This indicated that EC emission uncertainties in the sub-regions were substantial. Such uncertainty in the EC emission of each sub-region must be improved to obtain more accurate estimates of EC contributions and population exposure in South Korea.

Supplementary Information The online version contains supplementary material available at https://doi.org/10.1007/s11869-022-01213-z.

Author contribution Kyuwon Son: conceptualization, investigation, visualization, writing—original draft. Byeong-Uk Kim: conceptualization, writing—reviewing and editing. Hyun Cheol Kim: software, writing, reviewing and editing. Soontae Kim: writing—original draft; supervision.

Funding This work is financially supported by Korea Ministry of Environment (MOE).

Availability of data and material Source data are provided with the paper.

Declarations

Consent to publish The authors consent to publish.

Conflict of interest The authors declare no competing interests.

References

Andreae MO, Gelencser A (2006) Black carbon or brown carbon? The nature of light-absorbing carbonaceous aerosols. Atmos Chem Phys 6:3131–3148. https://doi.org/10.5194/acp-6-3131-2006

Apte JS, Marshall JD, Cohen AJ, Brauer M (2015) Addressing global mortality from ambient $PM_{2.5}$. Environ Sci Technol 49:8057–8066. https://doi.org/10.1021/acs.est.5b01236

Aunan K, Ma Q, Lund MT, Wang S (2018) Population-weighted exposure to $PM_{2.5}$ pollution in China: an integrated approach. Environ Int 120:111–120. https://doi.org/10.1016/j.envint.2018.07.042

Bae C, Kim EH, Yoo C et al (2021) Prioritizing local authorities effective to lower the nationwide PM2.5 concentrations and the personal exposure based on the source apportionment with the CAPSS 2016 emissions inventory. J Korean Soc 37:410–428. https://doi.org/10.5572/KOSAE.2021.37.3.410

Bae H, Lee S, Jung D, Oh G (2019) Study on the health effects of PM2.5 constituents for Health Risk Reduction Management Plan. KEI (Korea Environment Institute)

Binkowski FS, Roselle SJ (2003) Models-3 community multiscale air quality (CMAQ) model aerosol component 1. Model Description J Geophys Res 108:4183. https://doi.org/10.1029/2001JD001409

Byun D, Schere KL (2006) Review of the governing equations, computational algorithms, and other components of the models-3 community multiscale air quality (CMAQ) modeling system. Appl Mech Rev 59:51–77. https://doi.org/10.1115/1.2128636

Cao J, Xu H, Xu Q, Chen B, Kan H (2012) Fine particulate matter constituents and cardiopulmonary mortality in a heavily polluted Chinese City. Environ Health Perspect 120:373–378. https://doi.org/10.1289/ehp.1103671

Carter WPL (1999) Documentation of the SAPRC-99 mechanism for VOC reactivity assessment, draft final report on California Air Resources Board, Contracts No. 92–329 and 95–308

Chen B, Andersson A, Lee M et al (2013) Source forensics of black carbon aerosols from China. Environ Sci Technol 47:9102–9108. https://doi.org/10.1021/es401599r

Choi S, Kim T, Lee H et al (2020) Analysis of the national air pollutant emission inventory (CAPSS 2016) and the major cause of change in Republic of Korea. Asian J Atmos Enviro 14:422–445. https://doi.org/10.5572/ajae.2020.14.4.422

Dao, X., 2022. Significant reduction in atmospheric organic and elemental carbon in PM2.5 in 2+26 cities in northern China. Environmental Research 11.

Emery C, Liu Z, Russell AG, Odman MT, Yarwood G, Kumar N (2017) Recommendations on statistics and benchmarks to assess photochemical model performance. J Air Waste Manag Assoc 67:582–598. https://doi.org/10.1080/10962247.2016.1265027

Emery C, Tai E, Yarwood G (2001) Enhanced meteorological modeling and performance evaluation for two Texas ozone episodes, Prepared for the Texas Natural Resource Conservation Commission, by ENVIRON International Corporation 2001, p161. Available online: https://www.tceq.texas.gov/assets/public/implementation/air/am/contracts/reports/mm/EnhancedMetModelingAndPerformanceEvaluation.pdf. Accessed on 22 October 2018

Feng J, Zhong M, Xu B, Du Y, Wu M, Wang H, Chen C (2014) Concentrations, seasonal and diurnal variations of black carbon in PM2.5 in Shanghai, China. Atmos Res 147–148:1–9. https://doi.org/10.1016/j.atmosres.2014.04.018

Fisher BEA, Sokhi RS (2000) Investigation of roadside concentrations in busy streets using the model GRAM: conditions leading to high short-term concentrations. Int J Environ Pollut 14:488–495

Gu Z, Feng J, Han W, Li L, Wu M, Fu J, Sheng G (2010) Diurnal variations of polycyclic aromatic hydrocarbons associated with PM2.5 in Shanghai, China. J Environ Sci 22:389–396. https://doi.org/10.1016/S1001-0742(09)60120-0

Han C, Kim S, Lim Y-H, Bae H-J, Hong Y-C (2018) Spatial and temporal trends of number of deaths attributable to ambient PM2.5 in the Korea. J Korean Med Sci 33:1–14. https://doi.org/10.3346/jkms.2018.33.e193

Hart JE, Laden F, Eisen EA, Smith TJ, Garshick E (2009) Chronic obstructive pulmonary disease mortality in railroad workers. Occup Environ Med 66:221–226. https://doi.org/10.1136/oem.2008.040493

Heintzenberg J, Winkler P (1991) Elemental carbon in the atmosphere: challenges for the trace analyst. Fresenius' J Anal Chem 340:540–543. https://doi.org/10.1007/bf00322425

Huang L, Zhu Y, Zhai H, Xue S, Zhu T, Shao Y, Liu Z, Emery C, Yarwood G, Wang Y, Fu J, Zhang K, Li L (2021) Recommendations on benchmarks for numerical air quality model applications in China – part 1: PM2.5 and chemical species. Atmos Chem Phys 21:2725–2743. https://doi.org/10.5194/acp-21-2725-2021

Hong J-H, Jo YK (2003) The health effects of PM2.5: evidence from Korea. Environ Resour Econ Rev 12:469–485. (in Korean with English abstract)

Jang Y, Lee Y, Kim J, Kim Y, Woo J-H (2019) Improvement China point source for improving bottom-up emission inventory. Asia Pac J Atmos Sci 56:107–118. https://doi.org/10.1007/s13143-019-00115-y

Janssen NA, Hoek G, Simic-Lawson M et al (2011) Black carbon as an additional indicator of the adverse health effects of airborne particles compared with PM_{10} and $PM_{2.5}$. Environ Health Perspect 119:1691–1699. https://doi.org/10.1289/ehp.1003369

Jeong U, Kim J, Lee H, Jung J, Kim YJ, Song CH, Koo J-H (2011) Estimation of the contributions of long range transported aerosol in East Asia to carbonaceous aerosol and PM concentrations in Seoul, Korea using highly time resolved measurements: a PSCF model approach. J Environ Monit 13:1905. https://doi.org/10.1039/c0em00659a

Jia S, Zhang Q, Sarkar S et al (2020) Size-segregated deposition of atmospheric elemental carbon (EC) in the human respiratory system: a case study of the Pearl River Delta, China. Sci Total Environ 708:134932. https://doi.org/10.1016/j.scitotenv.2019.134932

Jo Y-J, Lee H-J, Jang L-S, Kim C-H (2017) Sensitivity study of the initial meteorological fields on the PM10 concentration predictions using CMAQ modeling. J Korean Soc Atmos Environ 33:554–569. https://doi.org/10.5572/KOSAE.2017.33.6.554

Keuken MP, Zandveld P, Jonkers S et al (2016) Modelling elemental carbon at regional, urban and traffic locations in the Netherlands. Atmos Environ 73:73–80. https://doi.org/10.1016/j.atmosenv.2013.03.010

Khan AJ, Li J, Husain L (2006) Atmospheric transport of elemental carbon. J Geophys Res 111:D04303. https://doi.org/10.1029/2005JD006505

Kiesewetter G, Borken-Kleefeld J, Schöpp W et al (2013) Modelling compliance with NO_2 and PM_{10} air quality limit values in the GAINS model. DG-Environment of the European Commission, Belgium, TSAP Report #9.

Kim S, Moon N, Byun D (2008) Korea emission inventory processing using the US EPA's SMOKE system.pdf. Asian J Atmos Environ 2:34–46

Kim S, Bae C, Kim E et al (2017) Domestic ozone sensitivity to Chinese emissions inventories: a comparison between MICS-Asia 2010 and INTEX-B 2006. J Korean Soc Atmos Environ 33:480–496. https://doi.org/10.5572/KOSAE.2017.33.5.480. (In Korean with English abstract)

Kim S, Kim O, Kim B-U, Kim HC (2017) Impact of emissions from major point sources in Chungcheongnam-do on surface fine particulate matter concentration in the surrounding area. KOSAE 33:159–173. https://doi.org/10.5572/KOSAE.2017.33.2.159

Kim B-U, Bae C, Kim HC, Kim E, Kim S (2017) Spatially and chemically resolved source apportionment analysis: case study of high particulate matter event. Atmos Environ 162:55–70. https://doi.org/10.1016/j.atmosenv.2017.05.006

Kim O, Bae M, Kim S (2020) Evaluation on provincial NOX and SO2 emissions in CAPSS 2016 based on photochemical model simulation. J Korean Soc Atmos Environ 36:64–83. https://doi.org/10.5572/KOSAE.2020.36.1.064. (In Korean with English abstract)

Kim S, You S, Kang Y-H, Kim E, Bae M, Son K, Kim Y, Kim B-U, Kim HC (2021) Municipality-level source apportionment of PM2.5 concentrations based on the CAPSS 2016: (II) Incheon. J Korean Soc Atmos Environ 37:144–168. https://doi.org/10.5572/KOSAE.2021.37.1.144

Krall JR, Anderson GB, Dominici F, Bell ML, Peng RD (2013) Short-term exposure to particulate matter constituents and mortality in a national study of U.S. urban communities. Environ Health Perspect 121:1148–1153. https://doi.org/10.1289/ehp.1206185

Kurokawa J, Ohara T, Morikawa T, Hanayama S, Janssens-Maenhout G, Fukui T, Kawashima K, Akimoto H (2013) Emissions of air pollutants and greenhouse gases over Asian regions during 2000–2008: Regional Emission inventory in ASia (REAS) version 2. Atmos Chem Phys 13:11019–11058. https://doi.org/10.5194/acp-13-11019-2013

Lee HS, Kang B-W (2001) Chemical characteristics of principal PM2.5 species in Chongju, South Korea. Atmos Environ 35:739–746. https://doi.org/10.1016/S1352-2310(00)00267-3

Lee S-G, Kim J-H, Kim S-S (2017) A case study of exposure to elemental carbon (EC) in an underground copper ore mine. J Environ Sci Int 26:1013–1021. https://doi.org/10.5322/JESI.2017.26.9.1013

Li K, Liao H, Mao Y, Ridley DA (2016) Source sector and region contributions to concentration and direct radiative forcing of black carbon in China. Atmos Environ 124:351–366. https://doi.org/10.1016/j.atmosenv.2015.06.014

Li J, Chen H, Li X, Wang M, Zhang X, Cao J, Shen F, Wu Y, Xu S, Fan H, Da G, Huang R, Wang J, Chan CK, De Jesus AL, Morawska L, Yao M (2019) Differing toxicity of ambient particulate matter (PM) in global cities. Atmos Environ 212:305–315. https://doi.org/10.1016/j.atmosenv.2019.05.048

Lim SS, Vos T, Flaxman AD et al (2012) A comparative risk assessment of burden of disease and injury attributable to 67 risk factors and risk factor clusters in 21 regions, 1990–2010: a systematic analysis for the Global Burden of Disease Study 2010. Lancet 380:2224–2260. https://doi.org/10.1016/S0140-6736(12)61766-8

Liu X, Bai X, Tian H et al (2020) Fine particulate matter pollution in North China: seasonal-spatial variations, source apportionment, sector and regional transport contributions. Environ Res 184:109368. https://doi.org/10.1016/j.envres.2020.109368

Lu Y, Shao M, Zheng C, Ji H, Gao X, Wang Q (2020) Air pollutant emissions from fossil fuel consumption in China: current status and future predictions. Atmos Environ 231:117536. https://doi.org/10.1016/j.atmosenv.2020.117536

Lu Y, Wang Q, Zhang X, Qian Y, Qian X (2019) China's black carbon emission from fossil fuel consumption in 2015, 2020, and 2030. Atmos Environ 212:201–207. https://doi.org/10.1016/j.atmosenv.2019.04.032

McMurry P. H., Shepherd M. H., Vickery J. S., (2004) Particulate matter science for policy makers A NARSTO Assessment

Morawska L, Hofmann W, Hitchins-Loveday J, Swanson C, Mengersen K (2005) Experimental study of the deposition of combustion aerosols in the human respiratory tract. J Aerosol Sci 36:939–957. https://doi.org/10.1016/j.jaerosci.2005.03.015

Mun J, Lee HW, Jeon W, Lee S-H (2017) Impact of meteorological initial input data on WRF simulation. J Environ Sci Int 26:1307–1319. https://doi.org/10.5322/JESI.2017.26.12.1307 (In Korean with English abstract)

National Air Pollutants Emission Service (NAIR) (2020) https://airemiss.nier.go.kr/user/boardList.do?command=view&page=1&boardId=160&boardSeq=559&id=airemiss_030500000000. Accessed 13 July 2021

National Air Pollutants Emission Service (NAIR) (2022) https://airemiss.nier.go.kr/user/boardList.do?command=view&page=1&boardId=160&boardSeq=559&id=airemiss_030500000000. Accessed 21 June 2022

Ogren JA, Charlson RJ (1984) Wet deposition of elemental carbon and sulfate in Sweden. Tellus B 36B:262–271. https://doi.org/10.3402/tellusb.v36i4.14908

Peng RD, Bell ML, Geyh AS et al (2009) Emergency admissions for cardiovascular and respiratory diseases and the chemical composition of fine particle air pollution. Environ Health Perspect 117:957–963. https://doi.org/10.1289/ehp.0800185

Petzold A, Ogren JA, Fiebig M et al (2013) (2013) Recommendations for the interpretation of "black carbon" measurements. Atmos Chem Phys 13:8365–8379. https://doi.org/10.5194/acp-13-8365-2013

Pierson WR, Brachaczek WW, McKee DE (1979) Sulfate emissions from catalyst-equipped automobiles on the highway. J Air Pollut Control Assoc 29:255–257. https://doi.org/10.1080/00022470.1979.10470790

Poschl U (2005) Atmospheric aerosols: Composition, transformation, climate, and health effects. Atmos Chem 44:7520–7540. https://doi.org/10.1002/anie.200501122

Qiao L, Cai J, Wang H, Wang W, Zhou M, Lou S, Chen R, Dai H, Chen C, Kan H (2014) PM 2.5 constituents and hospital emergency-room visits in Shanghai, China. Environ Sci Technol 48:10406–10414. https://doi.org/10.1021/es501305k

Qin Y, Xie SD (2012) Spatial and temporal variation of anthropogenic black carbon emissions in China for the period 1980–2009. Atmos Chem Phys 12:4825–4841

Rappazzo KM, Daniels JL, Messer LC, Poole C, Lobdell DT (2015) Exposure to elemental carbon, organic carbon, nitrate, and sulfate fractions of fine particulate matter and risk of preterm birth in

New Jersey, Ohio, and Pennsylvania (2000–2005). Environ Health Perspect 123:1059–1065. https://doi.org/10.1289/ehp.1408953

Rissler J, Swietlicki E, Bengtsson A et al (2012) Experimental determination of deposition 577 of diesel exhaust particles in the human respiratory tract. J Aerosol Sci 48:18–33. https://doi.org/10.1016/j.jaerosci.2012.01.005

Sahu LK, Kondo Y, Miyazaki Y, Pongkiatkul P, Kim Oanh NT (2011) Seasonal and diurnal variations of black carbon and organic carbon aerosols in Bangkok. J Geophys Res 116:D15302. https://doi.org/10.1029/2010JD015563

Shu Q, Koo B, Yarwood G, Henderson BH (2017) Strong influence of deposition and vertical mixing on secondary organic aerosol concentrations in CMAQ and CAMx. Atmos Environ 171:317–329. https://doi.org/10.1016/j.atmosenv.2017.10.035

Son K, Kim EH, Bae M et al (2020) Evaluations on $PM_{2.5}$ concentrations and the population exposure levels for local authorities in South Korea during 2015–2017. J Korean Soc Atmos Environ 36:806–819. https://doi.org/10.5572/KOSAE.2020.36.6.806 (In Korean with English abstract)

Streets DG, Bond TC, Carmichael GR, Fernandes SD, Fu Q, He D, Klimont Z, Nelson SM, Tsai NY, Wang MQ, Woo J-H, Yarber KF (2003) An inventory of gaseous and primary aerosol emissions in Asia in the year 2000: AEROSOL EMISSION INVENTORY. J Geophys Res 108. https://doi.org/10.1029/2002JD003093

Sung M, Moon K, Park J et al (2017) Chemical composition and source apportionment using the PMF model of the ambient $PM_{2.5}$ in 2013 over Korea. J Korean Soc Urban Environ 17:145–156 (In Korean with English abstract)

Tang R, Liu Q, Zhong W, Lian G, Yu H (2020) Experimental study of SO_2 emission and sulfur conversion characteristics of pressurized oxy-fuel co-combustion of coal and biomass. Energy Fuels 34:16693–16704. https://doi.org/10.1021/acs.energyfuels.0c03116

Thunis P, Degraeuwe B, Pisoni E et al (2018) PM2.5 source allocation in European cities: a SHERPA modelling study. Atmos Environ 187:93–106. https://doi.org/10.1016/j.atmosenv.2018.05.062

Viatte, C., Petit, J.-E., Yamanouchi, S., Van Damme, M., Doucerain, C., Germain-Piaulenne, E., Gros, V., Favez, O., Clarisse, L., Coheur, P.-F., Strong, K., Clerbaux, C., 2021. Ammonia and PM2.5 air pollution in Paris during the 2020 COVID lockdown. Atmosphere 12, 160. https://doi.org/10.3390/atmos12020160

Wang JM, Jeong C-H, Zimmerman N, Healy RM, Evans GJ (2018) Real world vehicle fleet emission factors: seasonal and diurnal variations in traffic related air pollutants. Atmos Environ 184:77–86. https://doi.org/10.1016/j.atmosenv.2018.04.015

Wang P, Wang H, Wang YQ et al (2016) Inverse modeling of black carbon emissions over China using ensemble data assimilation. Atmos Chem Phys 16:989–1002. https://doi.org/10.5194/acp-16-989-2016

Wang Y, Li L, Chen C et al (2014) Source apportionment of fine particulate matter during autumn haze episodes in Shanghai, China: source apportionment. J Geophys Res Atmos 119:1903–1914. https://doi.org/10.1002/2013JD019630

WHO. Health Effects of Black Carbon 2012. 96.

Wolff GT (1981) Particulate elemental carbon in the atmosphere. J Air Pollut Control Assoc 31:935–938. https://doi.org/10.1080/00022470.1981.10465298

Xing L, Li G, Pongpiachan S, Wang Q, Han Y, Cao J, Tipmanee D, Palakun J, Aukkaravittayapun S, Surapipith V, Poshyachinda S (2020) Quantifying the contributions of local emissions and regional transport to elemental carbon in Thailand. Environ Pollut 262:114272. https://doi.org/10.1016/j.envpol.2020.114272

Yu S, Dennis RL, Bhave PV, Eder BK (2004) Primary and secondary organic aerosols over the United States: estimates on the basis of observed organic carbon (OC) and elemental carbon (EC), and air quality modeled primary OC/EC ratios. Atmos Environ 38:5257–5268. https://doi.org/10.1016/j.atmosenv.2004.02.064

Zhang R, Tao J, Ho KF, Shen Z, Wang G, Cao J, Liu S, Zhang L, Lee SC (2012) Characterization of atmospheric organic and elemental carbon of PM2.5 in a typical semi-arid area of northeastern China. Aerosol and Air Quality Research 11